Kinetic Analysis of Oxygen Reduction on Pt(111) in Acid Solutions: Intrinsic Kinetic Parameters and Anion Adsorption Effects

J. X. Wang,*,† N. M. Markovic,‡ and R. R. Adzic†

Materials Science Department, Brookhaven National Laboratory, Upton, New York 11973, and Materials Science Division, Lawrence Berkeley National Laboratory, University of California, Berkeley, California 94720

Received: November 25, 2003; In Final Form: January 23, 2004

Oxygen reduction reaction (ORR) kinetics in acid solutions was studied by analysis of the polarization curves obtained by rotating disk electrode method for Pt(111) in $HClO_4$ and H_2SO_4 solutions. The model for ORR kinetic currents assumes that the intrinsic exchange current and Tafel slope are independent of anion adsorption. The site blocking and electronic effects of adsorbed OH (in $HClO_4$) and bisulfate (in H_2SO_4) were evaluated with the adsorption isotherms incorporated in the model. The best fits yielded the intrinsic Tafel slope in the range from −118 to −130 mV/dec, supporting single electron transfer in the rate-determining step with the corresponding transfer coefficients equal to 0.50 and 0.45, respectively. In addition to site blocking, a negative electronic effect on ORR kinetics was found for both OH and bisulfate with the effect of the latter being much stronger. The deviation of the apparent Tafel slope in $HClO_4$ from its intrinsic value can be fully accounted for by the site blocking and electronic effects of adsorbed OH ions, which vary with coverage over the mixed kinetic-diffusion controlled region. For Pt nanoparticle catalysts, the apparent Tafel slope is similar to that for Pt(111) in $HClO_4$ and the positive potential shift is mainly due to the increase in apparent exchange current as effective surface area increases.

1. Introduction

Oxygen reduction reaction is widely studied because it is the cathodic reaction in fuel cells, corrosion, and several other important processes.[1,2] From the catalytic point of view, the reaction mechanism on a Pt electrode has attracted most attention because Pt and Pt-alloys are still the most active catalysts for low-temperature fuel cells. In contrast to hydrogen oxidation on Pt, which is one of the very fast reactions, oxygen reduction on Pt exhibits slow and complicated kinetic behavior.

The standard reversible potential for O_2 reduction is 1.23 V on the hydrogen scale, but the oxygen cathode in a fuel cell has a working potential below 0.8 V so that there is a 400 mV potential loss, which is about 10 times larger than that for H_2 oxidation on anode. This large overpotential loss has been generally attributed to the sluggish kinetics of oxygen reduction reaction (ORR) and OH (from H_2O) or other anion adsorption. The latter was suggested based on the weak direct effect of the crystallographic orientation in $HClO_4$ and the strong indirect effect on the ORR kinetics in the H_2SO_4, H_3PO_4, and Cl^- containing solutions[3]. In the rotating ring-disk electrode (RRDE) studies of ORR in KOH, $HClO_4$, and H_2SO_4, Markovic and Ross[4] further demonstrated that the differences in the activity of three low index faces arise mainly from the structure-sensitive adsorption of anions. Although the negative effects of anion adsorption on ORR have been recognized, the features in the observed polarization curves have not been fully understood.

Some discussions were focused on the different apparent Tafel slopes observed for ORR on Pt electrodes in $HClO_4$ and H_2SO_4 solutions. As shown in Figure 1b, the curve for the H_2SO_4 solution (squares) can be fitted reasonably well with a Tafel slope of −118 mV/dec However, the $HClO_4$ curve (circles) deviates from the straight line with a −118 mV/dec slope at high potentials. In the sixties, this "low" Tafel slope at high potentials in $HClO_4$ solutions has been attributed to the Temkin conditions for the adsorption of reaction intermediates, mainly PtOH.[5] Later, several workers proposed that PtOH is not derived from the reduction of O_2, but rather from the reaction of H_2O with Pt, and that it causes inhibition of O_2 reduction.[6−8] Recently, Albu and Anderson[9,10] suggested that the cathodic

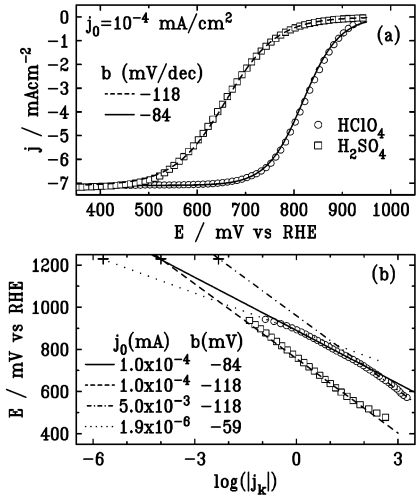

Figure 1. (a) Rotating disk electrode polarization curves for ORR on Pt(111) at 2500 rpm with a sweep rate of 50 mV/s in oxygen saturated 0.1 M $HClO_4$ (circles) and 0.05 M H_2SO_4 (squares) solution, obtained by averaging the absolute currents in both positive and negative sweep directions. The solid and dashed lines are fitted curves using eq 3 for the j_k in eq 2 as discussed in the text. (b) The Tafel plots for the data in (a) with the straight lines corresponding to different Tafel slopes and exchange currents.

* To whom correspondence should be addressed.
† Brookhaven National Laboratory.
‡ Lawrence Berkeley National Laboratory.

10.1021/jp037593v CCC: $27.50
Published on Web 03/05/2004

transfer coefficient, β, may vary with potential from about 0.5 to near 1.0 causing the Tafel slope changes from $-2.3RT/0.5F$ to $-2.3RT/F$ with increasing potential. This proposition, however, does not explain why the Tafel slope is potential independent for ORR on Pt(111) in H_2SO_4 solutions. Alternatively, Markovic et al.[11] proposed a model for the kinetic current, which assumes that the adsorbed OH can alter the adsorption energy of the ORR intermediates, thus has an energetic effect on ORR kinetics in addition to the site blocking. The OH coverage dependence of this energetic effect has been considered the main reason for the variation of the Tafel slope with potential for ORR on Pt(111) in $HClO_4$. Based on this assumption, the absence of OH adsorption in H_2SO_4 solution may explain why a single Tafel slope has been observed in H_2SO_4 but not in $HClO_4$ solutions. However, it is difficult to understand why only OH adsorption has an energetic effect on ORR, but not more strongly chemisorbed bisulfate.

To solve this puzzle, a model that can consistently explain the features in the rotating disk electrode (RDE) polarization curves in both solutions is needed. In this work, we developed such a model by defining the Tafel slope and the exchange current on an adsorbate-free Pt(111) surface as the intrinsic kinetic parameters and by taking into consideration both geometric site blocking and electronic effects of adsorbed anions. The adsorption isotherms for OH and bisulfate were obtained from the charges associated with their adsorption and incorporated in the analysis. By restraining the intrinsic kinetic parameters to the same values for the RDE polarization curves in both solutions, the anion adsorption effects were determined with respect to an adsorbate-free Pt surface. The results provide, not only the experimentally determined intrinsic kinetic parameters, but also a straightforward explanation as to why the apparent Tafel slope deviates from the intrinsic value in $HClO_4$ solutions.

2. Results and Discussions

2.1. Extracting ORR Kinetic Current from RDE Polarization Curves. Figure 1a shows the polarization curves for oxygen reduction on Pt(111) in $HClO_4$ and H_2SO_4 solutions obtained by using rotating disk electrode methods. Experimental details can be found in the previous publications.[11,12] Note that the maximum cathodic current densities are about the same (-7.1mA/cm^2) in both solutions and are close to the theoretical value for a four-electron reduction of O_2 in acid solutions at a rotation rate of 2500 rpm. Using this diffusion-limited current, j_l, as the diffusion-controlled current over the entire potential region (a valid approximation in most cases[13]), the kinetic current, j_k, can be obtained from eq 1, where j is measured current density

$$\frac{1}{j} = \frac{1}{j_k} + \frac{1}{j_l} \tag{1}$$

The data are shown in Figure 1b, where the potential is plotted as a function of the absolute value of the kinetic current, $j_k(E) = j_l\, j(E)/(j_l - j(E))$, in a semilogarithmic plot. This diffusion-corrected Tafel plot is often used to evaluate the Tafel slope, b, from the linear region of the curve.

Alternatively, the RDE polarization curves, $j(E)$, can be written as a function of $j_k(E)$, and j_l by rearranging eq 1

$$j(E) = \frac{j_k(E)}{1 + j_k(E)/j_l} \tag{2}$$

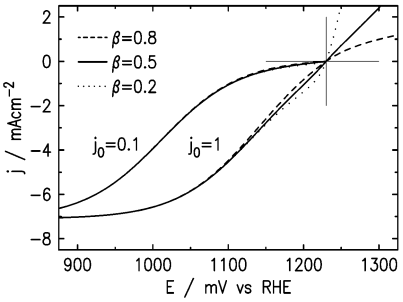

Figure 2. Calculated curves using eq 6 for the j_k in eq 2 with different β values for $b = -118$ mV/dec and $j_0 = 1$ or 0.1 mA/cm^2.

From the Tafel equation,[14] $\eta = E - E^\circ = b[\log |j_k| - \log(j_0)]$, the kinetic current for O_2 reduction can be expressed as

$$j_k = -j_0 \exp(2.303\eta/b) \tag{3}$$

where j_0 is the exchange current density over the geometric area of the electrode and $\eta = E - E^\circ$ is the overpotential. The Tafel slope, b, is expressed in mV per decade change of current density.

This *empirical* equation can be explained using absolute rate theory for an adsorbate-free surface. Assuming a linear dependence of the activation Gibbs energy, ΔG^* on overpotential, η, the kinetic current density for O_2 reduction is given by the Butler−Volmer equation

$$j_k = -j_0[\exp(-\beta nf\eta) - \exp((1-\beta)nf\eta)] \tag{4}$$

where the exchange current, j_0, is the preexponential factor of the absolute rate theory, β is the transfer coefficient for the cathodic reaction, n is the number of electrons transferred in the rate determining step for ORR, and $f = F/RT$. The second term represents a positive current due to the reversed reaction of ORR, which becomes negligible at large negative overpotentials. Thus, by combining the first term in eq 4 and eq 3, we have

$$-\beta nf = 2.303/b \tag{5}$$

Using this relationship, eq 4 can be rewritten as

$$j_k = -j_0\left[\exp(2.303\eta/b) - \exp\left(-2.303\eta/b\frac{1-\beta}{\beta}\right)\right] \tag{6}$$

To find under what conditions ORR kinetic currents can be described with sufficient accuracy by eq 3, six polarization curves were calculated by using eq 6 with different values for β and j_0, whereas b was fixed at -118 mV/dec As shown in Figure 2, all three curves obtained with β equal to 0.2, 0.5, and 0.8 overlap in the cathodic branch when $j_0 = 0.1$ mA/cm^2. For those with $j_0 = 1$ mA/cm^2, differences can be seen at small overpotentials in the cathodic branch. Since j_0 is smaller than 0.1 mA/cm^2 for ORR, β does not need to be treated as an independent parameter. Thus, eq 3 or the corresponding hyperbolic sine function, $j_k = -2j_0 \sinh(2.303\eta/b)$, were used to describe kinetic currents.[15]

The equation for calculating an ORR polarization curve was obtained by combining eqs 2 and 3. To fit the measured polarization curves, the Tafel slope and exchange current were allowed to vary, yielding $j_0 = 0.12$ and 0.15 μA/cm^2, $b = -86$ and -122 mV/dec for the $HClO_4$ and H_2SO_4 data shown in Figure 1a, respectively. Similar fitting quality can be obtained if $b = -118$ mV/dec was fixed in fitting of the H_2SO_4 data. The fitted j_0 is 0.10 μA/cm^2, slightly lower than the 0.15

μA/cm^2 value to compensate the difference in the Tafel slope. To simplify comparison, we then fixed j_0 at 0.1 μA/cm^2 in fitting the $HClO_4$ data, which yielded, $b = -84$ mV/dec The solid lines in Figure 1a show the curves calculated with these parameters. The agreements with the data are as good as those obtained by the best fits with both parameters free to vary. These facts indicate the Tafel slope and exchange current are strongly coupled. That is, one of the parameters can vary considerably if the other one is allowed to adjust accordingly. Both parameters should be determined for kinetic characterization of ORR activity. If the Tafel plot is used, the intercept of the straight line with the current axis at $E = E^0$ should give the exchange current as demonstrated in Figure 1b. Despite the uncertainty in each parameter due to the strong coupling between the Tafel slope and exchange current, the agreements with the data shown in Figure 1a indicate that there is no need for using the potential-dependent Tafel slope to describe the data.

Although these parameters are useful for numerical description of the kinetic currents, their physical interpretation based on the absolute rate theory might not be valid because of anion adsorptions in both solutions. Therefore, we refer to the kinetic parameters obtained by using the empirical Tafel equation (or eq 3) as the apparent kinetic parameters. Since OH adsorption from water on Pt at high potential cannot be eliminated in acid solutions, the intrinsic kinetic parameters for an adsorbate-free Pt surface have to be obtained through extrapolation. This will be discussed in the next section.

2.2. Intrinsic Kinetic Parameters and Adsorption Effects. To quantitatively evaluate the effects of adsorbed species on the ORR kinetics, the following pair of equations are derived from eq 3 with j_0* and b* as the *intrinsic* exchange current and Tafel slope for an adsorbate-free Pt(111) surface. A $(1 - \gamma\theta)^m$ term is added to account for the geometric site-blocking effect, whereas the electronic effect of anion adsorption on ORR kinetics is described by a coverage dependent potential shift through the exponential term, "$-\epsilon\theta$"

$$j_k(E) = -j_0^*(1 - \gamma_{OH}\theta_{OH}(E))^m \exp(2.303(E - E^0 - \epsilon_{OH}\theta_{OH}(E))/b^*) \quad (7)$$

$$j_k(E) = -j_0^*(1 - \gamma_A\theta_A(E))^m \exp(2.303(E - E^0 - \epsilon_A\theta_A(E))/b^*) \quad (8)$$

where γ and ϵ are the site-blocking and energy coefficients for either OH or the bisulfate anion (represented by OH and A, respectively) and m is the number of Pt sites involved in the rate determining step. To avoid model-dependent adsorption isotherms, we integrated the currents measured by linear sweep voltammetry in nitrogen-saturated solutions to obtain the potential dependent coverages, $\theta_{OH}(E)$ and $\theta_A(E)$.

In the model, the electronic effects of adsorbed anions are described by a coverage-proportional potential shift. This can be considered as a first-order approximation for the net effect due to all of the interactions. In general, the density functional calculations have shown that the activation energy at neighboring sites of an adsorbate may vary due to the direct (overlap of wave functions), indirect (shift of d electron states), elastic (substrate relaxation), and electrostatic (dipole) interactions.[16] Since induced dipole moments are in the same direction for anions and oxygen molecules, repulsive interactions and, hence, inhibition effects are expected.[17]

To obtain model-independent adsorption isotherms for analyses using eqs 7 and 8, the numerical results from measured charges were converted to analytic form as described below.

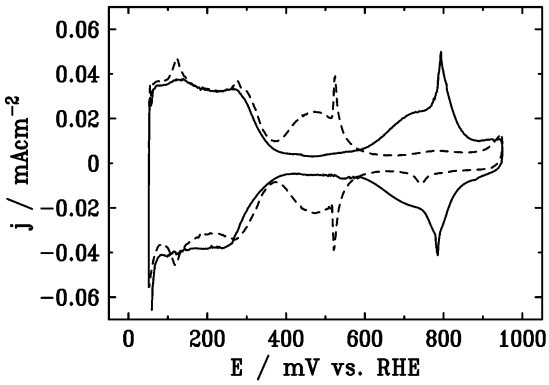

Figure 3. Linear sweep voltammetry curves for the Pt(111) electrode in nitrogen saturated 0.1 $HClO_4$ (solid line) and 0.05 M H_2SO_4 (dashed line) solutions. Sweep rate 50 mV/s.

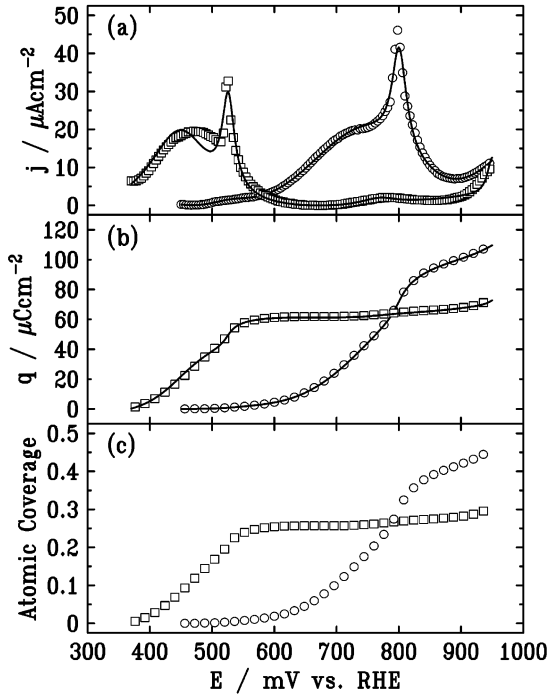

Figure 4. Currents (a), integrated charges (b), and atomic coverages (c) during a 50 mV/s positive potential sweep in nitrogen-saturated 0.1 M $HClO_4$ (circles) and 0.05 M H_2SO_4 (squares) solutions. The solid lines in (a) are the best fit by a function containing four Lorentzian peaks and linear background. The solid lines in (b) are calculated charge using the function with the fitting parameters, which are in good agreement with the results of numerical integration (circles and squares). Atomic coverage is calculated by normalization to the full monolayer coverage, 241 μC/cm^2, assuming one electron-transfer per adsorbate.

As shown in Figure 3, the current peaks in both curves are rather symmetric in the positive and negative directions and those at high potentials correspond to the anion adsorption and desorption, respectively. In $HClO_4$ solutions, the adsorbed anion is mainly OH from water dissociation, which occurs at potentials positive of 450 mV, whereas bisulfate adsorption occurs above 370 mV in H_2SO_4 solutions. Thus, the potential dependent OH coverage is obtained by integrating the current from 450 mV to E and normalized to the maximum charge at $E = 950$ mV, i.e., $\theta_{OH}(E) = \int_{450}^{E} j\,dE / \int_{450}^{950} j\,dE$. Similarly, the bisulfate adsorption isotherm is obtained by $\theta_A(E) = \int_{370}^{E} j\,dE / \int_{370}^{950} j\,dE$. To incorporate the potential-dependent coverage into eqs 7 and 8, analytic functions were deduced from the numerical data. The solid lines in Figure 4a show the best fits to the currents by a function containing four Lorentzian peaks and a linear

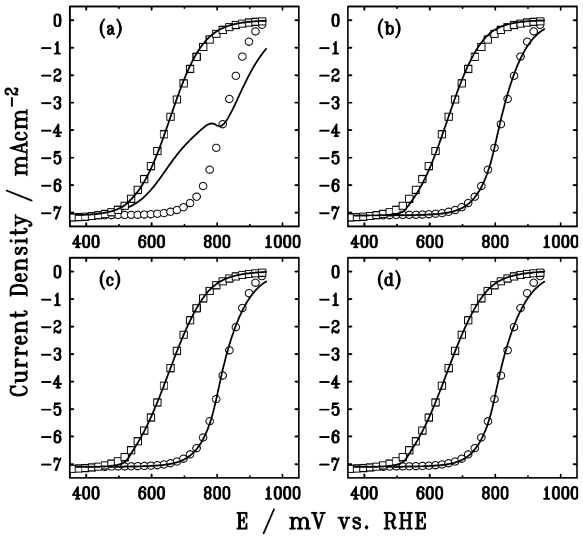

Figure 5. Best fits (solid lines) to the RDE polarization curves for ORR on Pt(111) in 0.1 M $HClO_4$ (circles) and 0.05 M H_2SO_4 (squares) solutions using different fixed parameters discussed in the text.

background. The charges as a function of potential, $q(E)$, calculated with the fitted parameters, are shown by the lines in Figure 4b, which reproduced the results obtained by numerical integration (symbols). Normalization to the maximum charge at the positive potential limit makes θ_{OH} and θ_A to vary between zero and unity over the corresponding potential regions. Thus, the site-blocking coefficient represents the maximum percentage of blocked sites at 950 mV. It should be equal to the maximum atomic coverage if the adsorbate to site blocking ratio is 1:1. To facilitate the discussion in the next section, the atomic coverages calculated from integrated charge with the assumption of one electron-transfer per adsorbate are shown in Figure 4c. Since 241 μC/cm^2 is needed for a full monolayer on Pt(111), the maximum atomic coverages are 0.46 and 0.3 monolayers for OH and bisulfate, respectively. Therefore, $\gamma_{OH} = {}^1/_2$ and $\gamma_A = 1/3$ are the reasonable values for fitting the polarization curves.

Based on eqs 7 and 8, three intrinsic kinetic parameters, j_0*, b*, and m should have the same values for fitting the two polarization curves. Besides these, there are two additional parameters for each of the two adsorbates. We first examine the assumption that bisulfate adsorption affects ORR kinetics only through site blocking, i.e., $\epsilon_A = 0$. A typical result for fitting with $\epsilon_A = 0$, $m = 2$, and $b^* = -118$ mV/dec is shown by the solid lines in Figure 5a. For the H_2SO_4 curve, agreement with the data can be obtained with $j_0^* = 0.18$ μA/cm^2 and $\gamma_A = 0.31$. However, with such a small exchange current, a large positive electronic effect ($\epsilon_{OH} = 243$ mV) is needed to shift the curve to more positive potentials. This electronic enhancement is unlikely and can be ruled out by the poor fit to the $HClO_4$ data.

To achieve good fits to both curves with meaningful parameters, we then chose to fit the $HClO_4$ curve first with $m = 2$, $b^* = -118$ mV/dec, and $\gamma_{OH} = 0.5$ while allowing j_0* and ϵ_{OH} to vary. Using the value obtained for j_0 from the fit for the $HClO_4$ curve, the fitting to the H_2SO_4 curve was carried out by letting both γ_A and ϵ_A to vary. The fits for both solutions, as shown in Figure 5b, are reasonably good. Further improvement can be obtained for the fitting to the H_2SO_4 data (reduced χ^2 error by half) by changing the value for the Tafel slope used in fitting. The best fit was obtained with $b^* = -130$ mV/dec as shown in Figure 5c, in which we also further restrain the site-blocking coefficient, γ_A, to be 0.33 because there is no

TABLE 1: Intrinsic Kinetic Parameters for ORR on Pt(111) Used in Equations 7 and 8 for the Fits Shown in Figure 5b−d and One Not Shown (#)[a]

curves	m	b^* (mV/dec)	j_0^* (μA/cm2)	γ_{OH}	ϵ_{OH} (mV)	γ_A	ϵ_A (mV)
b	2	−118	**7.7**	0.5	**−14**	**0.29**	**−230**
c	2	−130	**23**	0.5	**−42**	0.33	**−250**
d	1	−130	**25**	0.5	**−85**	0.33	**−278**
#	1	−118	**8.5**	0.5	**−53**	0.33	**−250**

[a] The bold faced values are varied to get the best fits with the other parameters fixed at the given values.

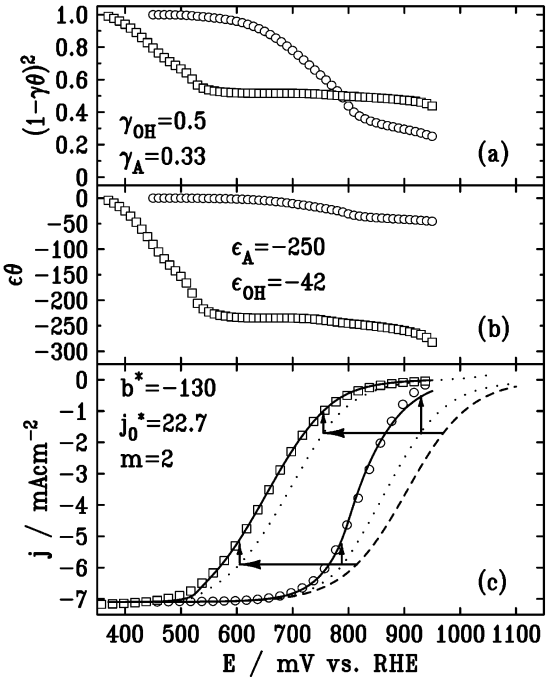

Figure 6. Potential dependence of site-blocking effect (a), potential shift due to electronic effects (b), and polarization curves in 0.1 $HClO_4$ (circles) and 0.05 M H_2SO_4 (squares) solutions (c). The solid lines are the fits to the data with the parameters given in the figure. The dashed line is calculated without any anion adsorption effects. The dotted lines include only the electronic effect. The upward arrows indicate the effect of site blocking by OH adsorption and the horizontal arrows show the negative potential shift due to electronic effects of adsorbed bisulfate ions.

apparent improvement by allowing this parameter to vary. At last, we show the fits with $b^* = -130$ mV/dec for $m = 1$ (Figure 5d). Similar fitting quality is also obtained with $b^* = -118$ mV/dec for $m = 1$ (not shown). All four sets of parameters are listed in Table 1.

The fitted parameter, j_0*, varies mainly with the Tafel slope, whereas the energy factors, ϵ_{OH} and ϵ_A, change with both b and m. Although some uncertainties remain for each parameter, the results clearly support the model, in which one electron transfer is involved in the rate-determining step with the transfer coefficient, β, equal to 0.5 or 0.45 for $b^* = -118$ or $b^* = -130$ mV/dec, respectively. Whether one or two Pt sites are involved in the rate-determining step cannot be unambiguously determined. Nevertheless, the intrinsic kinetic parameters and the anion adsorption effects are deconvoluted.

To illustrate the effect of anion adsorption on the ORR kinetics, the potential dependent site blocking, $(1 - \gamma\theta(E))^2$, and electronic, $\epsilon\theta(E)$, effects are plotted in Figure 6, parts a and b, together with the ORR polarization curves in Figure 6c. In H_2SO_4 solutions, the inhibition effects due to both the site blocking and electronic effect of the adsorbed bisulfate ions

increase quickly with increasing potential between 370 and 530 mV and are relatively constant at higher potentials. In contrast, the effects of OH adsorption vary with potential mainly in the potential region between 600 and 950 mV. The different behaviors result from the different adsorption isotherms (Figure 4c) since the major current peak for OH adsorption is at higher potential than that for bisulfate adsorption. By comparing Figure 6, parts a and b with part c, one can see that the major part of the mixed kinetic-diffusion controlled region for H_2SO_4 (500−900 mV) is above 530 mV, where the anion inhibition effects due to bisulfate adsorption are relatively *constant*. In contrast, the OH coverage, hence the inhibition effect *increases with increasing potential* over the entire mixed kinetic-diffusion controlled region for $HClO_4$ (600−900 mV). This is why the slope of the ORR polarization curve differs from its intrinsic value in $HClO_4$ but not in H_2SO_4.

Additional lines in Figure 6c provide further illustration. The dashed line is obtained with the intrinsic kinetic parameters without any adsorption effects and the dotted lines are calculated with the electronic effect included. The differences between the dashed and dotted lines show the electronic effect of adsorbed anions on the activation energy causing a potential shift indicated by the horizontal arrows. Since the solid lines include both the site-blocking and electronic effects whereas the dotted lines excludes the site-blocking effect, the differences between the two curves show the site blocking effects as marked by the vertical arrows. For $HClO_4$ solutions, both effects increase at higher potentials, which cause the slope of the ORR polarization curve, or the apparent Tafel slope, deviates from the intrinsic value. Since bisulfate adsorption saturates at a low potential, both site-blocking and electronic effects are nearly constant over the mixed kinetic-diffusion controlled region in H_2SO_4 solutions, and thus the apparent Tafel slope remains close to the intrinsic value.

2.3. From Ideal Model System to High Surface Area Real Catalysts, and to PE Fuel Cell. From studies of well-defined single-crystal electrode surfaces, we have demonstrated, in the previous section, that OH formation on Pt inhibits ORR and the variation of the OH coverage in the mixed kinetic-diffusion control region results in a deviation of the apparent Tafel slope from its intrinsic value. In this section, we show voltammetry and ORR polarization curves for Pt nanoparticles on a glassy carbon electrode in 0.1 M $HClO_4$ solution. Since it is difficult to accurately determine effective surface area and to have 100% utilization of a nanoparticle catalyst film, the discussion of the ORR reaction mechanism on Pt nanoparticles will be based on semiquantitative comparisons with the Pt(111) surface. In the end, we discuss the use of apparent kinetic parameters for kinetic characterization and the correlation between the kinetic parameters and catalyst performance tests in proton exchange fuel cells.

The Pt nanoparticles were obtained by combustion chemical-vapor deposition[18] and have a 13-nm average diameter. After sonification, 15 μL of slurry containing the unsupported Pt catalyst was transferred onto a 0.2 cm^2 glassy carbon rotating-electrode. The Pt loading was 0.1 mg/cm^2, corresponding to 500 nmol/cm^2. Since the percentage of atoms at the surface is roughly 10 for a 13-nm Pt particle, the nominal atomic density relative to geometric electrode area is 50 nmol/cm^2, which is 20 times of the atomic density of a Pt(111) surface.

The solid line in Figure 7a shows the voltammetry curve in nitrogen-saturated solution. It exhibits the characteristic feature for hydrogen adsorption on a polycrystalline Pt surface and the current is about 15 times that on a Pt(111) electrode (the dashed line with the current amplified by a factor 15 for comparison). This indicates that the effective surface area for the catalyst is about 15 times that on a smooth Pt(111) electrode, less than the 20-fold of nominal surface area relative to the Pt(111). The difference can be attributed to the blockage by direct contact of the nanoparticles. The appearance of the hydrogen adsorption/desorption feature in the ORR polarization curves shown in Figure 7b further suggests that this reaction occurs on a small part of the surface that is not utilized for ORR at large overpotentials because of the diffusion limitation of oxygen through the thin catalyst layer. This is likely to be the reason why the increase of exchange current discussed below is less than 15 times that for Pt(111).

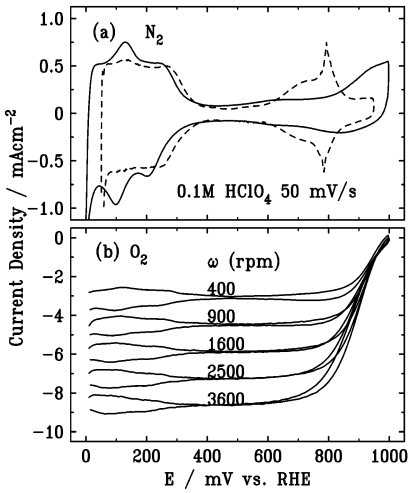

Figure 7. Linear sweep voltammetry in a 0.1 M $HClO_4$ solution (a) and ORR polarization curves at several rotating rates (b) for 13-nm Pt nanoparticles on a glassy carbon electrode with 0.1 mg/cm^2 loading (solid lines). The sweep rate is 50 mV/s. For comparison, the curve for the Pt(111) electrode in N_2 saturated solution is shown by the dashed line with the current enlarged by 15 times.

At more positive potentials, instead of the current peak for the OH monolayer formation on Pt(111), a gradual rise of the current with increasing potential from 400 to 800 mV is seen, followed by a sharp increase of current at potentials above 800 mV. This is not surprising since various Pt sites on a nanoparticle surface are likely to be oxidized at different potentials. The integrated charges for the positive potential sweeps in the voltammetry curves shown in Figure 7a are given in Figure 8a. By comparing them with the corresponding ORR polarization curves in Figure 8b, one can see that the major changes in OH-adsorption related charge for the Pt nanoparticle catalyst also occur in the mixed kinetic-diffusion control region. In addition, the slopes of the polarization curves are similar. These facts suggest that the reaction mechanism is essentially the same for both smooth and nanoparticle surfaces and that change of the OH coverage causes the apparent Tafel slope deviating from −118 mV/dec.

For a quantitative kinetic characterization, we have fitted the data in Figure 8b by using eq 3 for the kinetic current. The best fits yield the apparent kinetic parameters: $b = -91$ and −86 mV/dec and $j_0 = 1.31$ and 0.12 μA/cm^2 for the Pt nanoparticle and Pt(111), respectively. Note that since the effective surface area changes with the particle size and catalyst loading, the apparent kinetic parameters, especially the apparent exchange current, are sample specific. In the present case, the apparent exchange current for the nanoparticle catalyst sample is an order of magnitude higher than that for Pt(111), comparable to the 15 times larger hydrogen adsorption current discussed earlier. Thus, the high effective surface area is the major

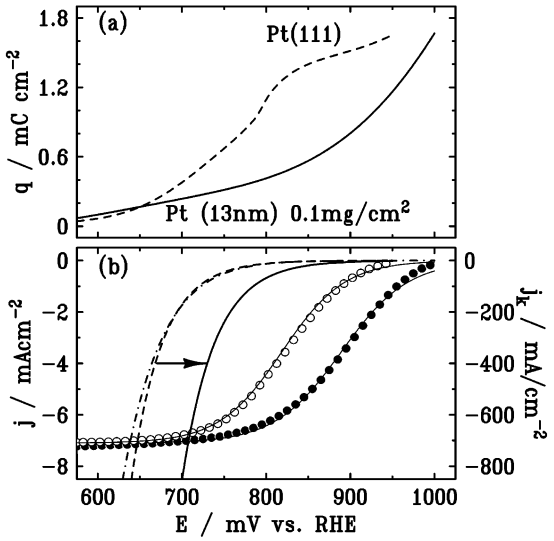

Figure 8. (a) Integrated charge as a function of potential in the positive potential sweep for the Pt nanoparticle catalyst (solid line) and the Pt-(111) electrode (dashed line, current enlarged by 15 times). (b) Polarization curves at 2500 rpm for Pt nanoparticles on a glassy carbon with 0.1 mg/cm^2 Pt loading (solid circles) and for Pt(111) (open circles) with the best fits (thin lines). The other three lines are the kinetic currents plotted against the right side current scale. The solid and dashed lines are calculated using eq 3 with the parameters obtained from the best fits for the Pt nanoparticle catalyst ($b = -91$ mV/dec and $j_0 = 1.31$ μA/cm^2) and the Pt(111) surface ($b = -86$ mV/dec and $j_0 = 0.12$ μA/cm^2), respectively. The dash−dot line is obtained by using eq 7 with $b^* = -118$ mV/dec, $j_0^* = 7.7$ μA/cm^2, $\gamma_{OH} = 0.5$, and $\epsilon_{OH} = -14$ mV. The arrow shows a 65 mV positive potential shift at −400 mA/cm^2 kinetic current.

contributor to the high apparent exchange current for the nanoparticle sample.

Using the apparent kinetic parameters obtained, the calculated kinetic currents as a function of potential for the two samples are shown in Figure 8b. For Pt(111), the kinetic current calculated from eq 7 with the intrinsic kinetic parameters is also shown. The difference between the two curves for Pt(111) (dashed and dot−dash lines) is visible but not so significant in terms of the potential difference at a constant current of −400 mA/cm^2 (see right side current scale). In comparison, the kinetic current for the Pt nanoparticle catalyst (solid line) reaches −400 mA/cm^2 at 730 mV, which is about 65 mV more positive than that for the Pt(111) surface. These results indicate that the reduction of 65 mV potential loss relative to a smooth Pt(111) surface is achieved mainly by an order of magnitude increase of the apparent exchange current through increasing the effective surface area.

At last, we show in Figure 9 the absolute value of kinetic current as a function of potential for ORR and hydrogen oxidation reaction (HOR) to illustrate the basic relationship between the results from RDE measurements and polymer electrolyte fuel cell testing. In a fuel cell stack test, a cell voltage is often measured as a function of current, which is equivalent to the potential difference between the two kinetic current curves at a given current in Figure 9. The two solid lines are generated for Pt(111) with the apparent kinetic parameters close to those obtained from analysis of the RDE polarization curves reported here for ORR and in another publication for HOR.[13] As shown by the arrows, the cell voltage at 400 mA/cm^2 is 668 − 74 = 594 mV. In practice, an order of magnitude higher apparent exchange currents can be achieved by using high surface area catalysts. The corresponding kinetic current curves are shown by the dashed lines and the cell voltage at 400 mA/cm^2 is

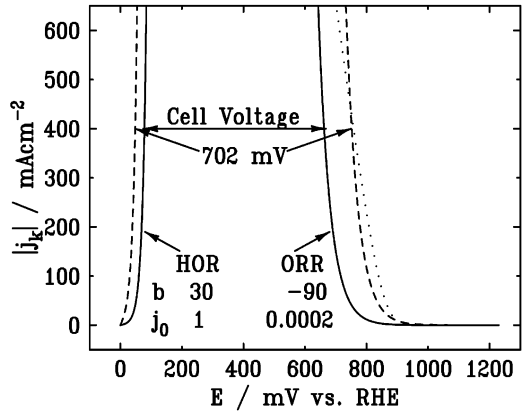

Figure 9. Absolute kinetic currents on Pt(111) as a function of potential (solid lines) calculated with the apparent kinetic parameters: $b = 30$ and −90 mV/dec, $j_0 = 1$ and 0.0002 mA/cm^2 for HOR and ORR, respectively. The dashed lines show the corresponding HOR and ORR curves with the same Tafel slopes but with 10 times larger exchange currents. The dotted line is calculated for the standard cathode-membrane polarization curve using the formula given in ref 19.

increased to 750 − 48 = 702 mV. The figure also illustrates that the voltage loss on the cathode for ORR (1228 − 750 = 478 mV) is about 10 times of that on the anode for HOR (48 mV). Focusing on the cathode, a cathode−membrane polarization curve calculated by using the formula given by Springer et al.[19] is shown by the dotted line for comparison with the cathode kinetic current curve (dashed line). The formula was developed empirically to include all of the voltage losses in a polymer electrolyte fuel cell operating at 80 °C except those on the anode. At low currents, the cathode−membrane polarization curve shows a smaller cathode voltage loss than the kinetic current curve (dashed line), whereas the opposite is seen at high currents. This behavior can be attributed to the higher catalytic activity at higher temperature (80 °C versus 25 °C), and an increase of a resistance-related voltage loss as the current increases. Overall, the figure shows the kinetic currents calculated from the apparent parameters obtained from RDE measurements at room-temperature correlate well to typical fuel cell testing results.

3. Conclusions

The intrinsic Tafel slope for ORR on Pt(111) was found in the range from −118 to −130 mV/dec at room temperature, supporting one-electron transfer in the rate-determining step with the transfer coefficient, β, being 0.50 or 0.45, respectively. The intrinsic exchange current is in the range from 7 to 25 μA/cm^2, depending on the Tafel slope and the number of Pt sites involved. In addition to the site-blocking effect, a negative electronic effect on ORR kinetics was found for both OH and bisulfate adsorption. Since the anion adsorption effects are proportional to the coverage, they affect the slope of the polarization curve only when the coverage changes in the mixed kinetic-diffusion controlled region for ORR. That is the reason why the apparent Tafel slope deviates from its intrinsic value in $HClO_4$ but not in H_2SO_4.

The ORR polarization curve obtained from nanoparticle Pt catalyst shifts positively compared to that from Pt(111), which can be attributed to the increase of apparent exchange current due to the larger effective surface area in the nanosized Pt particle catalyst. Similarities between the apparent Tafel slopes and the correlations with the voltammetry curves suggest that the reaction mechanism remains unchanged on nanoparticle surfaces. While keeping the apparent Tafel slope to be the same

as for Pt(111), an order of magnitude higher apparent exchange currents with respect to those found on Pt(111) were used to represent high surface area Pt catalysts. That is, with $b = 30$ and -90 mV/dec; $j_0 = 10$ and 0.002 mA/cm^2 for HOR on anode and ORR on cathode, respectively, a 0.7 V cell voltage was found at 0.4 A/cm^2 current, which is close to the typical result obtained in fuel cell testing.

Acknowledgment. This work is supported by U.S. Department of Energy, Divisions of Chemical and Material Sciences, under the Contract No. DE-AC02-98CH10886. N.M.M. acknowledges the support by the Director, Office of Science, Office of Basic Energy Sciences, Division of Materials Sciences, U.S. Department of Energy under Contract No. DE-AC03-76SF00098.

References and Notes

(1) Tarasevich, M. R.; Sadkowski, A.; Yeager, E. In *Kinetics and Mechanisms of Electrode Processes*; Conway, B. E., Bockris, J. O'M., Yeager, E., Khan, S. U. M., White, R. E., Eds.; Comprehensive Treatise of Electrochemistry; Plenum Press: New York, 1983; Vol. 7, pp 301−398.

(2) Adzic, R. R. In *Electrocatalysis*; Lipkowski, J., Ross, P. N., Eds.; Wiley-VCH: New York, 1998; pp 197−242.

(3) Kadiri, F. E.; Durand, R. *J. Electroanal. Chem*. **1991**, *301*, 177.

(4) Markovic, N. M.; Ross, P. N., Jr. In *Interfacial Electrochemistry, Theory, Experiment, and Applications*; Wieckowski, A., Ed.; Marcel Dekker: New York, 1999; p 821.

(5) Damjanovic, A.; Genshaw, M. A.; Bockris, J. O'M. *J. Phys. Chem*. **1964**, *45*, 4057.

(6) Tarasevich, M. R. *Elektrohimiya* **1973**, *9*, 578

(7) Adzic, R. R. In *Structural Effects in Electrocatalysis and Oxygen Electrochemistry*; Scherson, D. D., Tryk, D., Xing, X., Eds.; The Electrochem. Soc. Inc.: Pennington, 1992; Vol. 92−11, p 419.

(8) Uribe, F. A.; Wilson, M. S.; Springer, T. E.; Gottesfeld, S. In *Structural Effects in Electrocatalysis and Oxygen Electrochemistry*; Scherson, D. D., Tryk, D., Xing, X., Eds.; The Electrochem. Soc. Inc.: Pennington, 1992; Vol. 92−11, p 494.

(9) Albu, T. V.; Anderson, A. B. *Electrochim. Acta* **2001**, *46*, 3001.

(10) Sidik, R. A.; Anderson, A. B. *J. Electroanal. Chem*. **2002**, *528*, 69.

(11) Markovic, N. M.; Gasteiger, H. A.; Grgur, B. N.; Ross, P. N. *J. Electroanal. Chem.* **1999**, *467*, 157.

(12) Markovic, N. M.; Gasteiger, H. A.; Ross, P. N. *J. Phys. Chem*. **1995**, *99*, 3411.

(13) Wang, J. X.; Brankovic, S. R.; Zhu, Y.; Hanson, J. C.; Adzic, R. R. *J. Electrochem. Soc*. **2003**, *150*, A1108.

(14) Gileadi, E. In *Electrode Kinetics*; VCH Publishers: New York, 1993; p 108.

(15) In general, a hyperbolic sine function is preferred because it allows the current to approach zero at zero overpotential. Since we have checked that the error due to using simple exponential form is insignificant for ORR in this study, the simple exponential formula is used in discussion.

(16) Hammer B.; Norskov, J. K. *Adv. Catal.* **2000**, *45*, 71.

(17) Mortensen, J. J.; Hammer, B.; Norskov, J. K. *Phys. Rev. Lett*. **1998**, *80*, 4333.

(18) Leavitt, A. J.; Faguy, P. W. *Abstracts for 201st Meeting of The Electrochemical Society*; Electrochemical Society, Inc.: Pennington, NJ, 2001; abstract no. 128.

(19) Springer, T. E.; Zawodzinski, T. A.; Gottesfeld, S. *J. Electrochem. Soc.* **2001**, *148*, A11.